Journal of AI and Data Mining
Vol 8, No 4, 2020, 451-460. ***Original Research Paper*** DOI: 10.22044/JADM.2020.9131.2052

A Deep Model for Super-resolution Enhancement from a Single Image

N. Majidi, K. Kiani* and R. Rastgoo

Electrical and Computer Engineering Faculty, Semnan University, Semnan, Iran.

Received 28 November 2019; Revised 14 April 2020; Accepted 06 July 2020
**Corresponding author: Kourosh.kiani@semnan.ac.ir (K. Kiani).*

Abstract
This paper presents a method to reconstruct a high-resolution image using a deep convolution neural network. We propose a deep model, entitled Deep Block Super Resolution (DBSR), by fusing the output features of a deep convolutional network and a shallow convolutional network. In this way, our model benefits from the high frequency and low frequency features extracted from deep and shallow networks simultaneously. We use the residual layers in our model to make repetitive layers, increase the depth of the model, and make an end-to-end model. Furthermore, we employ a deep network in the up-sampling step instead of the bicubic interpolation method used in most of the previous works. Since the image resolution plays an important role to obtain rich information from the medical images and helps for an accurate and a faster diagnosis of the ailment, we use the medical images for resolution enhancement. Our model is capable of reconstructing a high-resolution image from a low-resolution one in both the medical and general images. The evaluation results on the TSA and TZDE datasets including MRI images, and Set5, Set14, B100, and Urban100 datasets including general images demonstrate that our model outperforms the state-of-the-art alternatives in both areas of medical and general super-resolution enhancement from a single input image.

Keywords: *Super Resolution, Residual Network, Medical Imaging, Enhancement, Deep Learning.*

1. Introduction

Image Super-Resolution (SR), the process of recovering high-resolution (HR) images from low resolution (LR) images, is an interesting area applicable to a wide range of real-world applications such as medical imaging [1-3], face recognition [4, 5], surveillance, and security [6]. This area is challenging because there are multiple HR images corresponding to a single LR input image. Generally, the SR methods can be classified into three categories: interpolation methods [4, 5], reconstruction-based methods [6-8], and learning-based methods [9-11]. The learning-based methods can be categorized into four groups: prediction-based methods, edge-based methods, statistical-based methods, and example-based methods [12]. Among these categories, the learning-based methods have attracted high research interests in the recent years with the advent of deep learning techniques. Deep learning has shown a prominent superiority over other machine learning algorithms in many artificial intelligence domains such as Computer Vision [13-15], Speech Recognition [16], and Natural Language Processing [17]. The models that use deep learning techniques cover the example-based group. In this paper, we propose a model using the deep convolutional neural network for the super-resolution enhancement from a single image.

The deep-based SR models have achieved the state-of-the-art performance on various benchmarks of SR [12]. Different deep learning methods, Convolutional Neural Network (CNN), and Generative Adversarial Net (GAN) have been applied to the SR area [SRCNN [18], SRGAN [19]]. In this way, we focus on a two-stream

model including a deep convolutional network for high frequency features parallel with a shallow network for low-frequency feature covering.

While CNN-based models for SR have achieved an outstanding performance [20], the existing models still have some shortcomings. First of all, most of them use fully convolutional neural networks that lead to failure to perceive the available information inside the image. Secondly, using a fixed interpolation kernel such as bicubic interpolation kernel function, only in post-processing stage is led to not adopting well during the image processing. Thus it can decrease the quality of the reconstructed image [21]. In order to address these problems, in this work, we used a CNN-based model including a deep network parallel with a shallow network to obtain both the low- and high-frequency information from the input image. Furthermore, we use a deep model to adopt the interpolation kernel instead of using a fixed interpolation kernel function. Our contributions are listed as follows:

- We employed a deep network in the up-sampling step instead of the bicubic interpolation method used in most of the previous works.
- A two-stream network including a deep network and a shallow network is proposed to push both the low- and high-frequency information simultaneously from an input image.
- We used the residual layers to make a repetitive layer, increase the depth of the model, and make an end-to-end model.
- Our model outperforms the state-of-the-art alternatives in super-resolution enhancement from both the medical and general images.

The rest of this paper is organized as what follows. The related works are introduced in Section 2. The proposed model is described in detail in Section 3. The experimental results are provided in Section 4. Finally, we conclude the paper in Section 5.

2. Related Works

Here, we present a brief review of the recent works in SR enhancement from a single image input in the example-based category, in which deep learning has an effective role. Dong *et al*. have proposed a Super-Resolution Convolutional Neural Network (SRCNN) including four layers. They proved that using a larger CNN filter size was better than using deeper CNN layers in the Single Image Super Resolution (SISR) tasks [3]. Kim *et al*. have designed a Deeply-Recursive Convolutional Network for Image Super Resolution (DRCN) using 20 CNN layers and huge numbers of parameters. They used a sharing mechanism in order to decrease the training parameters and enhance the model performance. The evaluation results of the model showed that the model achieved significant performances on the Set5, Set14, B100, and Urban100 datasets [4]. Using Deep Residual Learning [6] and gradient clipping, Very Deep Super Resolution (VDSR) developed a way to make a training step with a significantly fast capability [5]. Mao *et al*. have also used residual learning to propose a very deep Residual Encoder-Decoder Networks (RED) including the symmetric convolutional (encoder) and de-convolutional (decoder) layers to improve the SR accuracy. Benefiting from the symmetric structure and skip connections, RED could train a very deep network including large numbers of convolutional layers. The evaluation results on the BSD200 and Set14 datasets showed a better performance than the previously reported state-of-the-art methods [7]. Romano *et al*. have developed a Rapid and Accurate Image Super Resolution (RAISR) model including a shallow and faster learning-based method. They used the patch angle, strength, and coherence to classify the input image patches and make a learning process to map from LR image to HR image among the clustered patches. The experimental results on the Set5 and Set14 datasets demonstrated that the model had a higher performance in comparison with the state-of-the-art models [8]. Dong *et al*. have designed a faster version of SRCNN, namely Faster-SRCNN, using the transposed CNN to directly process the input image [9]. While the processing speed of the RAISR and FRSCNN models is 10 to 100 times faster than the other state-of-the-art Deep Learning based methods, they are not as accurate as the other deeply convolutional methods like DRCN, VDSR or RED. In order to make an enhancement in this area, in this work, we applied a deep convolutional model for SR enhancement from an input image considering the following issues:

• Previous works used a deep or a shallow model to feature extraction. In this work, we used both the deep and shallow networks simultaneously to obtain the high- and low-frequency features of a low-resolution image.

• We employed the residual layers to make a

repetitive layer and increase the depth of the model to have more strong features.

• The previous works used a fixed interpolation kernel such as bicubic interpolation kernel function only in the post-processing stage that can lead to not adopting well during the processing. Thus it could decrease the quality of the reconstructed image.

In this way, we used the residual layers in the up-sampling process instead of using the previous methods (for example bicubic) and made an end-to-end model.

3. Model

In this section, we present the details of our model according to the steps shown in Figure 1.

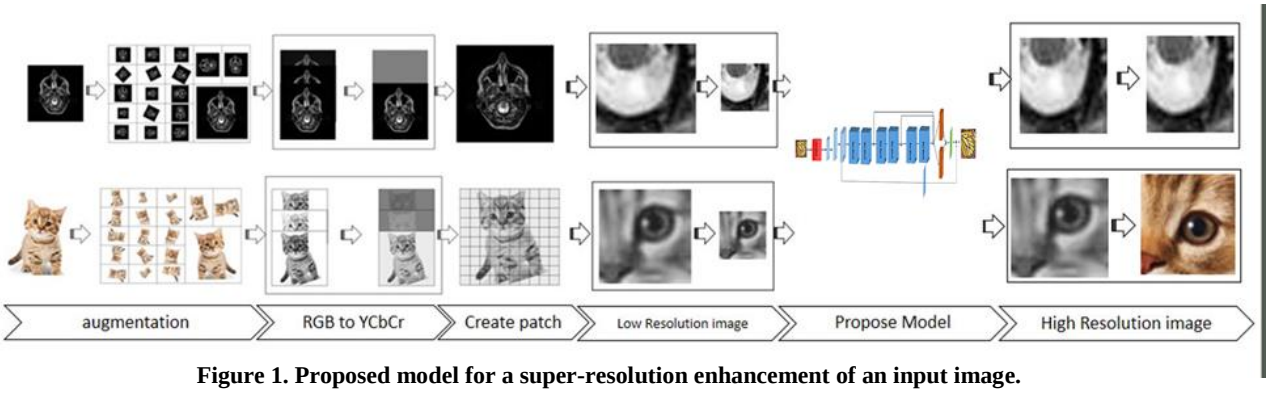

Figure 1. Proposed model for a super-resolution enhancement of an input image.

3.1. Augmentation

In order to extend the dataset samples, provide a large dataset applicable in the deep learning area, and prevent overfitting, we applied some augmentation techniques to the input data; they were scaling up/down using different scale factors and rotating using different rotation angles.

3.2. RGB to YCbCr

While the RGB space includes three color channels, Red, Green, and Blue, the YCbCr space contains Gray, Blue, and Green. We transferred the input RGB image to the YCbCr space to process it. In this way, we did the training process on the Gray channel and added the other channels to the image in the last step. This helped us to work with only one channel in the training phase instead of all channels in the RGB space.

3.3. Patching

Due to using an example-based model, we are required to have some patches from an input image. In order to provide these patches with the 48x48 dimension, we used the low-resolution input patches with 12x12, 16x16, and 24x24 shapes. After that, we applied a bicubic interpolation method with three scale factors (4, 3, 2) to these patches. In this way, we had some patches with the 48x48 dimension that would be sent to a deep and a shallow model to enhance the resolution. The labels according to the original low-resolution image would be assigned to these patches.

3.4. Deep Model

We proposed a deep model, DBSR, shown in the third row of figure 2 including a combination of the deep and shallow networks to benefit from this combination in order to obtain both the high- and low-frequency features. Our model includes three parts as follows, as shown in figure2:

- **Shallow network:** This network contains two convolutional layers; the first convolutional layer is similar to the one used in deep network. The input shape of this layer is 48x48 with a filter size of 3x3. The second layer with an input shape of 48x48 and the filter size of 3x3 is used to reconstruct the high-resolution image from the input low-resolution patches.
- **Deep network:** This network includes two parts. The first part, the feature extraction block, contains six residual blocks. Each block contains three layers: Convolutional, ReLU, and Dropout layers, with an input shape of 48x48, a filter size of 3x3, and a depth of 64. The outputs of the residual blocks are sent to the construction layer to process and obtain a high resolution image. The

second part is a reconstruction block including two parallel convolutional layers with a depth of 64 and one convolutional layer with a depth of 1. The input shape and filter size of these layers are similar to the other layers.

- **Reconstruction block:** We fuse the outputs of the deep and shallow networks to reconstruct a high resolution image. Different fusion types such as Max, Conv., and Sum are tested to select the best one. Since the Sum fusion gets the better results in the proposed model, we use it in the proposed model.

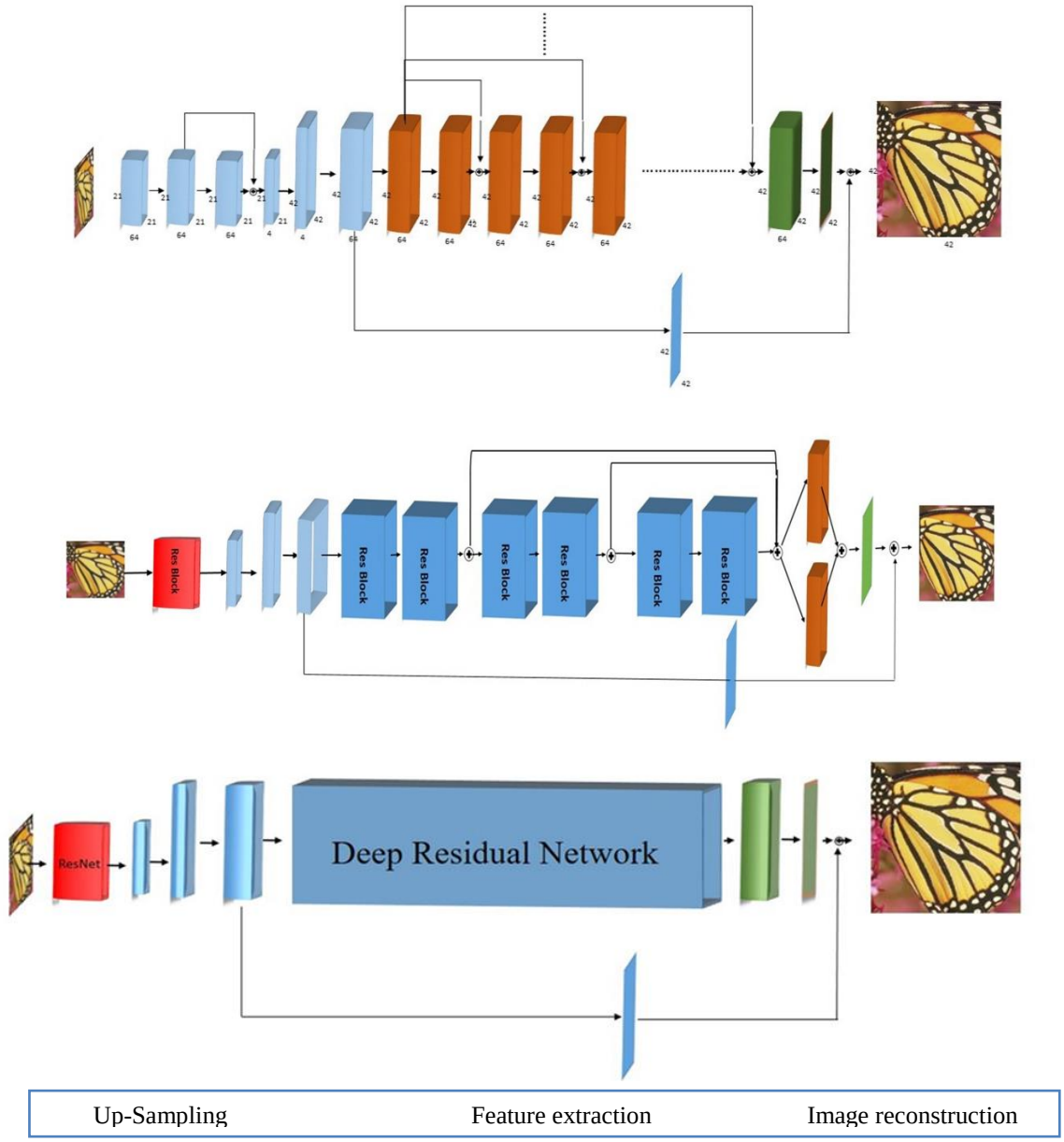

Figure 2. Architecture of the proposed model. First row: SCRSR, Second row: RBSR, Third row: DBSR.

4. Results

In this section, we report the experimental results of our model on the public datasets.

4.1. Implementation Details

Our evaluations were done on Intel(R) Xeon(R) CPU E5-2699 (2 processors) with 60GB RAM on Microsoft Windows 10 operating system on NVIDIA GPU, Tesla K80. We used Stochastic Gradient Descent (SGD) with a mini-batch size of 64. The learning rate starts with 0.00001. The proposed model is trained for a total 200 epochs. For fair comparisons with existing models, we used the same training and testing sets employed in the datasets used for evaluation. We used three scaling factors (2, 3, 4) for the performance evaluation of the proposed model.

4.2. Datasets

We used eight datasets in two categories for our model evaluation, as follow:

- Medical datasets: In this category, we used three datasets: T2, TSA, TZTD. The T2 dataset including the 732 MRI samples is used for model training. Our model was evaluated on the TSA and TZTD datasets with 27 and 28 MRI images.
- General datasets: In this category, we used 291 datasets including 291 samples of different images from different categories for model training. Evaluation was done on the Set5, Set14, B100, and Urban100 datasets with 5, 14, 100, and 100 image samples. Figure 3 demonstrates some samples of these datasets. To sum up, we trained our model on the T2 and 291 datasets for the medical and general input images. Using the augmentation methods, we extended these datasets to include 6221 and 5372 samples. After patching phase, we had 513462 and 632206 patches in two datasets. The proposed model was separately trained with each of the three scaling factors used in our evaluation.

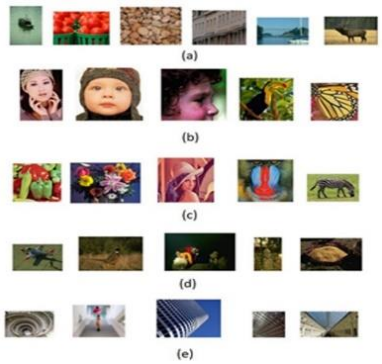

Figure 3. Some samples of the datasets used in our model: (a): dataset 291, (b): dataset SET5, (c): dataset SET14, (d): dataset B100, (e): dataset Urban 100.

4.3. Evaluation Metrics

In order to have a fair comparison with the other models, we used two metrics to report the results, as follow:

- PSNR**:** In the image super-resolution, Peak Signal-to-Noise Ratio (PSNR) [22] is defined via the maximum possible pixel value and the Mean Squared Error (MSE) [22] between images.
- **SSIM:** The Structural Similarity (SSIM) [18] metric is used to measure the structural similarity between images using three parameters, namely luminance, contrast, and structure.

4.4. Comparison Results

We performed an analysis on our model in five datasets used in the test phase. As one can see in tables 1-4, we have the highest performance on the Set 5 [23], Set 14 [24], Urban 100 [25], BSD100 [26], and T2 [27] datasets using the PSNR and SSIM metrics with three scale factors. Furthermore, we visualized some samples to compare with the other models.

Based on the evaluation results, we achieved a higher performance by increasing the depth of the model using the residual blocks. Furthermore, the fusion type and location of deep and shallow networks are so important and effective. In this way, we proposed three models, shown in figure 2, and compared them to select a more accurate one. Using the deep residual network instead of using some residual blocks is led to a higher performance. We performed a detailed analysis on the three proposed models, namely Skip Connection Resnet Super Resolution (SCRSR), Resnet Block Super Resolution (RBSR), and DBSR in order to select a more accurate model. The evaluation results of these models are reported in table 1-4.

In order to evaluate and verify the efficiency and reliability of the proposed model in terms of providing sufficiently illustrative information from low resolution images, we compared our model with the state-of-the-art models on the five datasets used for evaluation, shown in table 1-4. As these tables confirm, our model outperforms the state-of-the-art alternatives in the field.

Benefiting from the extracted low- and high-frequency information simultaneously using a two-stream network, our model obtains a higher performance using different evaluation metrics and input image categories on five public datasets. Furthermore, we employed a deep network in the up-sampling step instead of the bicubic interpolation method used in most of the previous works. In this way, our model can learn the up-sampling phase instead of only using a fixed and pre-defined interpolation kernel. In addition, while we are training the model, we either train the layers in the residual blocks or skip the training for those layers using skip connections. In this way, we have a faster training step for our model. For all of these reasons, our model obtains a higher performance on five datasets.

Table 1. Evaluation results on the T2 dataset using PSNR metric and scale factor 2.

Model	TZDE	TSA	T2
Bicubic	32.19	32.35	30.49
SRCNN [18]	35.65	36.11	33.86
EEDS [34]	35.76	36.58	34.28
SCRSR (ours)	36.48	37.51	35.29
RBSR (ours)	36.58	37.68	35.40
DBSR (ours)	**36.68**	**37.92**	**35.72**

Table 2. Evaluation results on the T2 dataset using SSIM metric and scale factor 2.

Model	TZDE	TSA	T2
Bicubic	0.963	0.9445	0.9433
SRCNN [18]	0.9088	0.9488	0.9316
EEDS [34]	0.9791	0.9536	0.956
SCRSR (ours)	0.988	0.9694	0.9727
RBSR (ours)	0.9872	0.9719	0.9745
DBSR (ours)	**0.9876**	**0.9703**	**0.9731**

Table 3. Evaluation results on four datasets using PSNR metric and three scale factors 2, 3, and 4.

Dataset	**Set 5**			**Set 14**			**BSD 100**			**Urban100**		
Scale	X2	X3	X4	X2	X3	X4	X2	X3	X4	X2	X3	X4
Bicubic	33.66	30.39	28.42	30.24	27.55	26.00	29.56	27.21	25.96	24.95	23.56	22.98
SUSR [24]	35.78	31.90	29.69	31.81	28.67	26.88	30.40	27.15	25.92	-	-	-
A+ [28]	36.55	32.59	30.29	32.28	29.13	27.32	30.78	28.18	26.77	-	-	-
ARFL [29]	36.71	32.57	30.21	32.36	29.12	27.31	31.26	28.28	26.79	-	-	-
NBSRF [30]	36.76	32.75	30.44	32.45	29.25	27.41	31.30	28.36	26.88	-	-	-
SRCNN [18]	36.34	32.39	30.09	32.18	29.00	27.20	31.11	28.20	26.70	28.23	27.76	26.98
SRCNN-L [31]	36.66	32.75	30.49	32.45	29.30	27.50	31.36	28.41	26.90	-	-	-
CSC [32]	36.62	32.66	30.36	32.31	29.16	27.30	31.27	28.31	26.83	-	-	-
CSCN [33]	36.93	33.10	30.86	32.56	29.41	27.64	31.40	28.50	27.03	-	-	-
EEDS [34]	37.29	33.47	31.14	32.81	29.60	27.82	31.64	28.64	27.11	28.05	27.12	26.26
SCRSR (ours)	37.98	33.89	31.76	33.24	30.22	28.46	32.05	28.98	27.88	28.86	27.86	27.04
RBSR (ours)	38.70	34.24	32.12	33.98	30.82	28.98	32.48	29.24	28.14	28,90	27.98	27.22
DBSR (ours)	**39.38**	**34.86**	**32.92**	**34.64**	**31.34**	**29.24**	**32.88**	**29.98**	**28.78**	**29.46**	**28.32**	**27.86**

Table 4. Evaluation results on four datasets using SSIM metric and three scale factors 2, 3, and 4.

Dataset	**Set 5**			**Set 14**			**BSD 100**			**Urban 100**		
Scale	X2	X3	X4	X2	X3	X4	X2	X3	X4	X2	X3	X4
Bicubic	0.9299	0.8682	0.8104	0.8687	0.7736	0.7019	0.8431	0.7385	0.6675	0.8268	0.8124	0.8012
SUSR [24]	0.9493	0.8968	0.8428	0.8988	0.8075	0.7342	0.8682	0.7695	0.6968	-	-	-
A+ [28]	0.9544	0.9088	0.8603	0.9056	0.8188	0.7491	0.8773	0.7808	0.7085	-	-	-
ARFL [29]	0.9548	0.9077	0.8565	0.9059	0.8181	0.7465	0.8864	0.7825	0.7066	-	-	-
NBSRF [30]	0.9552	0.9104	0.8632	0.9071	0.8212	0.7511	0.8876	0.7856	0.7110	-	-	-
SRCNN [18]	0.9521	0.9033	0.8530	0.9039	0.8145	0.7413	0.8835	0.7794	0.7018	0.9034	0.8922	0.8898
SRCNN-L [31]	0.9542	0.9090	0.8628	0.9067	0.8215	0.7513	0.8879	0.7863	0.7103	-	-	-
CSC [32]	0.9548	0.9098	0.8607	0.9070	0.8209	0.7499	0.8876	0.7853	0.7101	-	-	-
CSCN [33]	0.9552	0.9144	0.8732	0.9074	0.8238	0.7578	0.8884	0.7885	0.7161	-	-	-
EEDS [34]	0.9579	0.9191	0.8783	0.9105	0.8284	0.7626	0.8928	0.7925	0.7200	0.8993	0.8902	0.8824
SCRSR (ours)	0.9588	0.9197	0.8798	0.8971	0.8292	0.7634	0.8934	0.7936	0.7212	0.9110	0.9056	0.9044
RBSR (ours)	0.9592	0.9202	0.8804	0.8965	0.8298	0.7640	0.8950	0.7944	0.7226	0,9140	0.9089	0.9054
DBSR (ours)	**0.9612**	**0.9234**	**0.8836**	**0.8964**	**0.8330**	**0.7692**	**0.8998**	**0.7992**	**0.7288**	**0.9156**	**0.9092**	**0.9062**

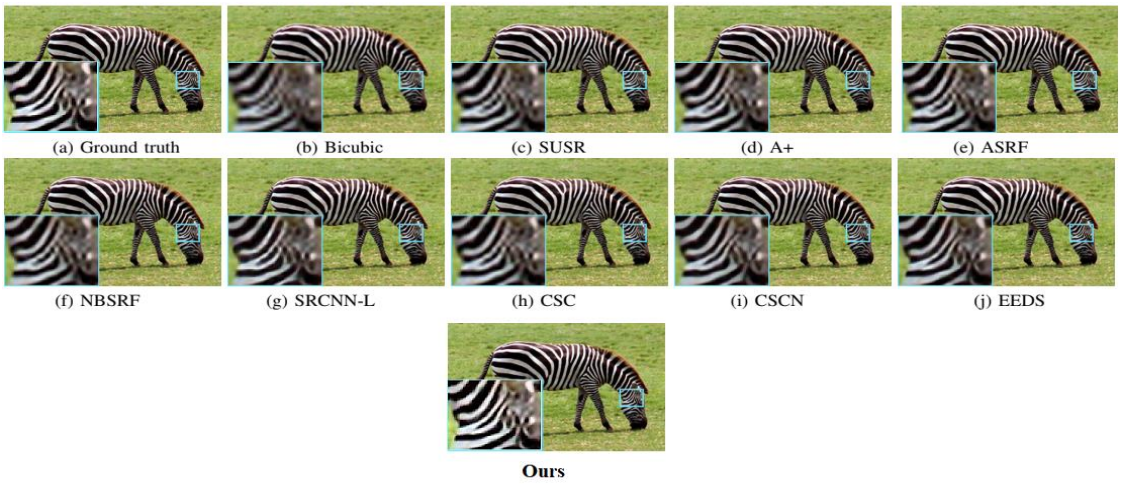

Figure 4. The "barbara" image from Set 14 with an upscaling factor of 3.

Figure 5. The "comic" image from Set 14 with an upscaling factor of 3.

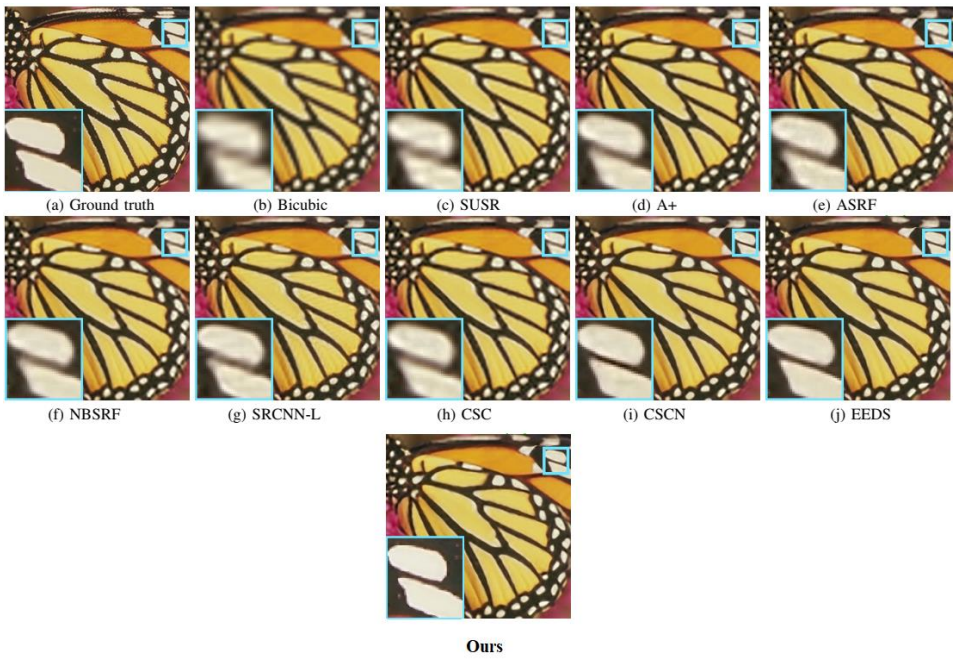

Figure 6. The "butterfly" image from Set 5 with an upscaling factor.

5. Conclusions and Discussion

In this work, we proposed a model to enhance the performance of the super-resolution form a single input image. We fused two networks, a shallow and a deep one, to simultaneously benefit from the capability of a shallow network in low-frequency feature extraction and high-frequency feature extraction of deep network. Despite the previous works, we used a deep network including residual blocks to do the up-sampling phase of our model. While the evaluation results of our model on five datasets in the medical and general areas demonstrated that this model outperformed the state-of-the-art models in both areas, much more endeavours are necessary to obtain the outputs with a higher resolution quality. Since the image resolution plays an important role to obtain the important information from the medical images and helps for an accurate and a faster diagnosis of the ailment, we are required to enhance the image resolution much more. We need other deep models such as GAN in our model to obtain a higher model performance.

References

[1] Greenspan, H. (2008). Super-resolution in medical imaging. Computer Journal, vol. 52, no. 1, pp. 43-63. DOI: https://doi.org/10.1093/comjnl/bxm075

[2] Isaac, J.S. & Kulkarni, R. (2015). Super resolution techniques for medical image processing. International Conference on Technologies for Sustainable Development (ICTSD), Mumbai, India, 2015. DOI: 10.1109/ICTSD.2015.7095900.

[3] Huang, Y., Shao, L. & Frangi, A.F. (2017). Simultaneous super-resolution and cross-modality synthesis of 3d medical images using weakly-supervised joint convolutional sparse coding. IEEE International Conference on Computer Vision (CVPR), Hawaii, United States, 2017.

[4] Lin, F., Fookes, C., Chandran, V. & Sridharan, S. (2007). Super-resolved faces for improved face recognition from surveillance video. International Conference on Biometrics (ICB), Seoul, Korea, 2007.

[5] Rasti, P., Uiboupin, T., Escalera, S. & Anbarjafari, Gh. (2016). Convolutional neural network super resolution for face recognition in surveillance monitoring. International Conference on Articulated Motion and Deformable Objects (AMDO), Palma de Mallorca, Spain, 2016.

[6] Zhang, L., Zhang, H., Shen, H. & Li, P. (2010). A super-resolution reconstruction algorithm for surveillance images. Signal Processing, vol. 90, no. 3, pp. 848-859. https://doi.org/10.1016/j.sigpro.2009.09.002.

[7] Dai, D., Wang, Y., Chen, Y. & Van Gool, L. (2016). Is image super-resolution helpful for other vision tasks? IEEE Winter Conference on Applications of Computer Vision (WACV), Lake Placid, NY, USA, 2016.

[8] Zhang, H., Liu, D. & Xiong, Z. (2018). Convolutional neural network-based video super-resolution for action recognition. 13th IEEE International Conference on Automatic Face & Gesture Recognition (FG 2018), Xi'an, China, 2018.

[9] Haris, M., Shakhnarovich, G. & Ukita, N. (2018). Task-driven super resolution: Object detection in low-resolution images. Arxiv: 1803.11316.

[10] Sajjadi, M.S., Scholkopf, B. & Hirsch, M. (2017). Enhancement: Single image super-resolution through automated texture synthesis. IEEE International Conference on Computer Vision (ICCV), Venice, Italy, 2017.

[11] Zhang, Y., Bai, Y., Ding, M. & Ghanem, B. (2018). Sod-mtgan: Small object detection via multi-task generative adversarial network. European Conference on Computer Vision (ECCV), Munich, Germany, 2018. DOI: https://doi.org/10.1007/978-3-030-01261-8_13.

[12] Yang, Ch. Y., Ma, Ch. & Yang, M. H. (2014). Single-Image Super-Resolution: A Benchmark, European Conference on Computer Vision (ECCV), Zurich, Switzerland, 2014. DOI: https://doi.org/10.1007/978-3-319-10593-2_25.

[13] Rastgoo, R., Kiani, K. & Escalera, S. (2020). Hand sign language recognition using multi-view hand skeleton, Expert Systems with Applications, nol. 150, no. 113336. DOI: https://doi.org/10.1016/j.eswa.2020.113336.

[14] Rastgoo, R., Kiani, K. & Escalera, S. (2018). Multi-Modal Deep Hand Sign Language Recognition in Still Images Using Restricted Boltzmann Machine. Entropy 2018, vol. 20, no. 809.

[15] Rastgoo, R., Kiani, K. & Escalera, S. (2020). Video-based isolated hand sign language recognition using a deep cascaded model, Multimedia Tools and Applications. DOI: https://doi.org/10.1007/s11042-020-09048-5.

[16] Asadolahzade Kermanshahi, M. & Homayounpour, M.M. (2019) Improving Phoneme Sequence Recognition using Phoneme Duration Information in DNN-HSMM. Journal of AI and Data Mining (JAIDM), vol. 7, no. 1, pp. 137-147.

[17] Torfi, A., Shirvani, R.A., Keneshloo, Y., Tavaf, N. & Fox, E.A. (2020). Natural Language Processing Advancements by Deep Learning: A Survey. ArXiv: 2003.01200v2.

[18] Chao Dong, Ch., Change-Loy, Ch., He, K. & Tang, X. (2014). Learning a deep convolutional network for image super-resolution. Proceedings of

European Conference on Computer Vision (ECCV), Zurich, Switzerland, 2014. DOI: https://doi.org/10.1007/978-3-319-10593-2_13.

[19] Ledig, C., Theis, L., Huszar, F., Caballero, J., Cunningham, A. & et al. (2017). Photorealistic single image super-resolution using a generative adversarial network. IEEE International Conference on Computer Vision (CVPR), Hawaii, United States, 2017. DOI: 10.1109/CVPR.2017.19.

[20] Wang, Zh., Chen, J. & Hoi, S.C.H. (2020). Deep Learning for Image Super-resolution: A Survey. arXiv:1902.06068v1.

[21] Michaeli, T. & Irani, M. (2013). Nonparametric blind super-resolution. In: IEEE International Conference on Computer Vision (CVPR), Portland, Oregon, 2013.

[22] Horé, A. & Ziou, D. (2010). Image Quality Metrics: PSNR vs. SSIM, 20th International Conference on Pattern Recognition, Istanbul, Turkey, 2010.

[23] Bevilacqua, M., Roumy, A., Guillemot, C. & Alberi-Morel, M.-L. (2012). Low-complexity single-image super-resolution based on nonnegative neighbor embedding. British Machine Vision Conference (BMVC) 2012, pp. 1–10.

[24] Zeyde, R., Elad, M. & Protter, M. (2010). On single image scale-up using sparse-representations. International Conference on Curves and Surfaces, Avignon, France, 2010. DOI: https://doi.org/10.1007/978-3-642-27413-8_47.

[25] Huang, J.B., Singh, A. & Ahuja, N. (2015). Single Image Super-Resolution from Transformed Self-Exemplars. Proceedings of the IEEE Conference on Computer Vision and Pattern Recognition, Massachusetts, USA, 2015.

[26] Martin, D., Fowlkes, C., Tal, D. & Malik, J. (2001). A database of human segmented natural images and its application to evaluating segmentation algorithms and measuring ecological statistics. Proceedings of IEEE International Conference on Computer Vision, Canada, vol. 2, 2001, pp. 416–423.

[27] Structural MRI Datasets (2020), Available: https://www.kaggle.com/ilknuricke/neurohackinginrimages.

[28] Timofte, R., Smet, V.D. & Gool, L.V. (2014). A+: Adjusted anchored neighborhood regression for fast super-resolution. Proceedings of Asian Conference on Computer Vision (ACCV), Singapore, 2014. DOI: https://doi.org/10.1007/978-3-319-16817-3_8.

[29] Schulter, S., Lesistner, C. & Bischof, H. (2015). Fast and accurate image upscaling with super-resolution forests. Proceedings of IEEE Conference on Computer Vision and Pattern Recognition (CVPR), Boston, Massachusetts, USA, 2015. DOI: 10.1109/CVPR.2015.7299003.

[30] Salvador J. & Pérez-Pellitero, E. (2015). Naive Bayes super-resolution forest. Proceedings of IEEE International Conference on Computer Vision (CVPR), Santiago, Chile, 2015. DOI: 10.1109/ICCV.2015.45.

[31] Dong, Ch., Loy, Ch. Ch., He, K. & Tang, X. (2016). Image super-resolution using deep convolutional networks. IEEE Transactions on Pattern Analysis and Machine Intelligence, vol. 38, no. 2, pp. 295–307. DOI: 10.1109/TPAMI.2015.2439281.

[32] Gu, S., Zuo, W., Xie, Q., Meng, D., Feng, X. & Zhang, L. (2015). Convolutional sparse coding for image super-resolution. Proceedings of IEEE International Conference on Computer Vision (ICCV), Santiago, Chile, 2015. DOI: 10.1109/ICCV.2015.212.

[33] Wang, Z., Liu, D., Yang, J., Han, W. & Huang, T. (2015). Deep networks for image super-resolution with sparse prior. Proceedings of IEEE International Conference on Computer Vision (ICCV), 2015. DOI: 10.1109/ICCV.2015.50.

[34] Wang, Y., Wang, L., Wang, H. & Li, P. (2019). End-to-End Image Super-Resolution via Deep and Shallow Convolutional Networks. IEEE Access, Vol. 7, pp. 31959 – 31970. DOI: 10.1109/ACCESS.2019.2903582.